



# Egomotion-related visual areas respond to goal-directed movements

Martina Bellagamba<sup>1,2</sup> · Valentina Sulpizio<sup>2,3</sup> · Patrizia Fattori<sup>4</sup> · Gaspare Galati<sup>2,3</sup> · Claudio Galletti<sup>4</sup> · Teresa Maltempo<sup>1,2</sup> · Sabrina Pitzalis<sup>1,2</sup>

Received: 9 December 2021 / Accepted: 4 June 2022 / Published online: 28 June 2022  
© The Author(s), under exclusive licence to Springer-Verlag GmbH Germany, part of Springer Nature 2022

## Abstract

Integration of proprioceptive signals from the various effectors with visual feedback of self-motion from the retina is necessary for whole-body movement and locomotion. Here, we tested whether the human visual motion areas involved in processing optic flow signals simulating self-motion are also activated by goal-directed movements (as saccades or pointing) performed with different effectors (eye, hand, and foot), suggesting a role in visually guiding movements through the external environment. To achieve this aim, we used a combined approach of task-evoked activity and effective connectivity (PsychoPhysiological Interaction, PPI) by fMRI. We localized a set of six egomotion-responsive visual areas through the flow field stimulus and distinguished them into visual (pIPS/V3A, V6+, IPSmot/VIP) and visuomotor (pCi, CSv, PIC) areas according to recent literature. We tested their response to a visuomotor task implying spatially directed delayed eye, hand, and foot movements. We observed a posterior-to-anterior gradient of preference for eye-to-foot movements, with posterior (visual) regions showing a preference for saccades, and anterior (visuomotor) regions showing a preference for foot pointing. No region showed a clear preference for hand pointing. Effective connectivity analysis showed that visual areas were more connected to each other with respect to the visuomotor areas, particularly during saccades. We suggest that visual and visuomotor egomotion regions can play different roles within a network that integrates sensory–motor signals with the aim of guiding movements in the external environment.

**Keywords** Visuomotor control · Superior parietal lobule · Pointing · Functional magnetic resonance · Optic flow

## Introduction

For whole-body movement and locomotion, we need to appropriately use sensory and motor inputs to maintain balance and to reach (or avoid) specific objects or locations in space. Specifically, when we move and perform

goal-directed movements (as saccades or pointing), proprioceptive signals from the various effectors (eye, hand, or foot) need to be merged with visual feedback of self-motion from the retina (known as the optic flow; Gibson 1950) to visually guide our movements through the external environment. Whether this interaction occurs in the same visual cortical areas responding to optic flow or in other sensory motor cortices is still an open question.

Human neuroimaging studies have revealed multiple cortical areas responding to egomotion-compatible optic flow stimuli, located in occipital, temporal, parietal, cingulate, and insular cortices (Cardin and Smith 2010; Pitzalis et al. 2010, 2013a, b, 2019; Serra et al. 2019; Wall and Smith 2008). Among them, six areas (V3A, V6+, VIP, pCi, CSv, and PIC) can be consistently defined at an individual level with egomotion-compatible stimulation like the flow field stimulus (Serra et al. 2019).

The *visual* properties of these regions have been deeply investigated in recent years, and a comparison of their functional profiles reveals several commonalities but also

---

Martina Bellagamba and Valentina Sulpizio have contributed equally to this work.

---

✉ Sabrina Pitzalis  
sabrina.pitzalis@uniroma4.it

- <sup>1</sup> Department of Movement, Human and Health Sciences, University of Rome ‘‘Foro Italico’’, 00194 Rome, Italy
- <sup>2</sup> Department of Cognitive and Motor Rehabilitation and Neuroimaging, Santa Lucia Foundation (IRCCS Fondazione Santa Lucia), Rome, Italy
- <sup>3</sup> Brain Imaging Laboratory, Department of Psychology, Sapienza University, Rome, Italy
- <sup>4</sup> Department of Biomedical and Neuromotor Sciences, University of Bologna, Bologna, Italy

some differences. Some of these regions respond to changing heading directions (V6+, VIP, pCi and CSv: Di Marco, et al. 2021a, b; Furlan et al. 2014; PIC: Huang et al. 2015), are specialized in distinguishing among different types of self-movement (V6+ and VIP: Pitzalis et al. 2013a, b), show vestibular responses and appear to integrate visual and vestibular cues to estimate self-motion (VIP and PIC: Billington and Smith 2015; Greenlee et al. 2016; Smith et al. 2012, 2017), contribute to perceptual stability during pursuit eye movements (V3A and V6: Fischer et al. 2012; Galletti et al. 1990; Galletti and Fattori 2003; Nau et al., 2018), and could be involved in the “flow parsing” mechanism (Galletti and Fattori 2018; Warren and Rushton 2009). Most of them process self-motion cues from different sense modalities (Greenlee et al. 2016).

Although most of these previous human functional MRI (fMRI) studies have focused on the visual role of these egomotion-sensitive areas, based on their sensitivity to egomotion-compatible optic flow, in recent years, it has been gaining ground the idea that some of these areas also play a motor role (Smith 2021; Smith et al. 2018). The general hypothesis is that these visual regions might respond also during motor actions performed when moving in a dynamic environment to visually guide our limb movements during walking. Notably to this regard, in a recent fMRI study, we tested the sensitivity of these areas to a pure motor task requiring to actively perform long-range arm and leg movements (Serra et al. 2019). We revealed that, while the egomotion cortical regions V3A, V6+, and IPSmot do not respond to long-range leg movements (visual areas), the egomotion areas pCi, CSv, and PIC respond to both optic flow and long-range leg movements (visuomotor areas) and are also connected to sensorimotor cortices where lower limbs are represented.

Within the same framework, it is plausible to hypothesize the possible contribution of these visually defined egomotion cortical areas in the control of goal-directed movements. Although most of the human studies on the neural bases of goal-directed movements, as saccades or hand pointing, focus on the Posterior Parietal Cortex (PPC), there are also evidence of the involvement in saccades of V3A (e.g., Sereno et al. 2001) and V6+ (e.g., Tosoni et al. 2015). A few human fMRI studies (Heed et al. 2011, 2016; Leone et al. 2014; Medendorp and Heed 2019; Pitzalis et al. 2019) tested three effectors, comparing activity during memory guided eye, hand, and foot movements. The whole-brain maps shown in these studies revealed a wide network of cortical areas activated by the three types of pointing movements including not only lateral intraparietal areas, known for being involved in saccades or reaching planning, but also cingulate, insular, and medial parietal areas where egomotion-related areas responding to optic flow are located. However, besides the whole-brain maps, these studies did not

perform a regional analysis on the egomotion regions, leaving open the question of their effector-dependent involvement in goal-directed movements.

In the current study, we examined the response to goal-directed movements of six egomotion regions defined using the Flow Field stimulus by analyzing brain activations from a Pointing/Saccade task (previously published in Pitzalis et al. (2019) implying spatially directed delayed eye, hand, and foot movements. Specifically, we tested whether these six egomotion regions exhibit distinct patterns of activity with respect to the three effectors used in the Pointing/Saccade task. Based on Serra et al. (2019) showing that the three visuomotor regions (pCi, CSv, and PIC) are activated by a pure motor task implying long-range leg movements (Serra et al. 2019), we hypothesized that pCi, CSv, and PIC are activated even when using foot pointing movements directed toward different spatial locations in the visual field.

Finally, to verify whether the dynamic interactions between these six egomotion regions during the execution of pointing movements are effector-dependent, we also examined the pattern of functional connectivity of the egomotion-sensitive areas as estimated through a PsychoPhysiological Interaction (PPI) approach (Friston et al. 1997). Table 1 lists all the acronyms used in the paper to indicate the egomotion regions.

## Materials and methods

### Participants

The present study is based on a reanalysis of BOLD data from a sub-sample of subjects ( $N = 18$ , 10 females, mean age 25.22 years, SD 3.39 years) who participated in a previous study from our lab (Maltempo et al. 2021; Pitzalis et al. 2019). One subject of the original sample was excluded, because he did not undergo the visual motion task. All participants had normal or corrected-to-normal vision and no previous history of psychiatric or neurologic disease. Hand and foot right-dominance were tested by the Edinburgh

**Table 1** The acronyms (and their meaning) used in the paper to indicate the egomotion regions are provided

Acronym	Meaning
V6+	V6 complex
pIPS/V3A	Posterior intraparietal sulcus/V3A
PSmot/VIP	Intraparietal area motion area/ ventral intraparietal area
pCi	Posterior cingulate area
CSv	Cingulate sulcus area
PIC	Posterior insular cortex

handedness inventory (Oldfield 1971). All volunteers had given their written informed consent to participate, and the original studies had been approved by the research ethics committees at Fondazione Santa Lucia in Rome, according to the Declaration of Helsinki.

## Stimuli and experimental paradigm

Each participant underwent (1) a localizer session, consisting of a visual motion stimulation paradigm hereafter called flow fields, designed to map six egomotion regions (pIPS/V3A, V6+, IPSmot/VIP, pCi, CSv, and PIC; Fig. 1A) according to Serra et al. (2019) and (2) a visuomotor task (delayed saccades and hand/foot pointing; Fig. 1B) designed to reveal the responsiveness of the six egomotion regions to spatially directed pointing movements and to isolate effector-preference representations in the parietal cortex.

1. Localizer for the six egomotion ROIs (Flow Fields scans). A description of this stimulus is provided in detail elsewhere (e.g., Pitzalis et al. 2010; Serra et al. 2019; see also Fig. 1A). Participants passively observed eight 16-s blocks of coherently moving dot fields (dilations, contractions, spirals, and rotations), interleaved with eight 16-s blocks of randomly moving dot fields, while maintaining central fixation. A new field of white dots was generated every 500 ms (dot size  $0.4 \times 0.4 \text{ deg}^2$ ) and the stimulus was presented in full view. Dots immediately began to move along a trajectory to generate a coherent movement on a plane. The motion pattern was chosen randomly for that 500 ms period from a continuum ranging from dilation to outward spiral, rotation, inward spiral, and contraction. The center of the movement was jittered from flow to flow, and the dot speed was logarithmically scaled with eccentricity (average speed:  $25^\circ/\text{s}$ ; range of speed variance:  $17\text{--}33^\circ/\text{s}$ ). During the scrambled OFF period, dots and their movement vectors were generated as during the coherent ON periods except that each dot trajectory was rotated by a

random angle around the pattern center before execution. This scrambled the coherency of movement (at a given point, dots moved in different directions) but preserved the speed gradient (central dots still moved slower than peripheral dots).

2. Pointing/Saccade task. Participants performed a visuomotor task implying spatially directed delayed eye, hand, and foot movements toward different spatial locations within the visual field. A detailed description of this task is provided in Pitzalis et al. (2019); see also Fig. 1B. Each trial began with observers maintaining central fixation while holding a button down with their right index and a foot pedal down with their right foot. Each block started with a written instruction (“Fix”, “Eye”, “Hand”, and “Foot”) appearing for 400 ms in the center of a screen to inform the subject about the task to be performed, followed by four trials (Fig. 1B). On each trial, a peripheral target (a white dot of diameter 0.9 deg in size) indicating the location for the upcoming movement appeared for 300 ms in one of eight different angular positions (30, 60, 120, 150, 210, 240, 300, and 330 deg) at an eccentricity of 4 deg of visual angle. Targets were distributed along a circle whose center corresponded to the center of the screen (i.e., the fixation point) and arranged as in a clock. During each block, target locations appeared in a random order. After a variable delay (1.5, 2.5, 3.5 or 4.5 s), the fixation point turned green (go signal) for 300 ms and participants either moved the eyes while continuing to hold button and pedal (eye blocks) or released the button/pedal and rotated their wrist/ankle (without moving the shoulder/leg) to point toward the remembered target location with their right index/toe while keeping central fixation (hand/foot pointing blocks). Subjects were instructed to immediately return to the resting position after movement execution. Visual stimuli were back projected onto a screen positioned behind the subjects’ head and visible through a mirror above the head coil. In this way, targets appeared as if they were positioned in front of the

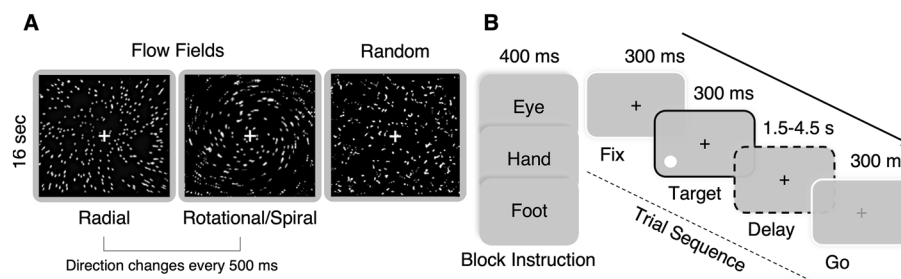


**Fig. 1** Experimental tasks. **A** Visual motion task. Blocks of coherently moving dot fields (flow fields) were interleaved with blocks of randomly moving dot fields. **B** Pointing/Saccade task. Subjects alter-

nated blocks of memory delayed saccadic and hand/foot pointing movements to peripheral visual targets with passive fixation blocks

subjects, just above their heads. To allow participants to rotate the limb in the direction cued by the target, we placed a cylindrical cushion to support their wrist/ankle, so as they could rotate their right index/toe toward all the possible ‘remembered’ target locations. Before starting the experiment, participants performed a short warm-up within the scanner to familiarize themselves with the task and the movement directions. Note that we asked participants to perform very short-range pointing movements and they reported being able to rotate their joints to point toward the spatial locations previously indicated by the target. Although we could not track movements during the scanning session, we did not expect any effect related to the direction of movement into the ipsilateral or contralateral visual field in our regions of interest. Indeed, in a previous fMRI study based on the same pool of data (Maltempo et al. 2021), we did not find any difference, at the whole-brain level, between activations elicited by ipsilateral and contralateral targets.

3. Each scan included four saccades, four hand pointing and four foot pointing blocks lasting 18 s each, arranged in a pseudo-random sequence and interleaved with 11 fixation periods of variable duration (12, 14, or 16 s).

## Apparatus and procedure

Functional images were acquired using a 3T Siemens Allegra MR System (Siemens Medical systems, Erlangen, Germany) equipped for echo-planar imaging with a standard head coil and operating at the Neuroimaging Laboratory, Foundation Santa Lucia. Visual stimuli were presented by a control computer located outside the MR room, running in-house software (Galati et al. 2008) implemented in MATLAB (The MathWorks Inc., Natick, MA, USA). We used an LCD video projector with a customized lens to project visual stimuli to a projection screen positioned at the back of the MR tube. The timing of presentation of each stimulus was controlled and triggered by the acquisition of fMRI images.

We used blood-oxygenation level-dependent imaging (Kwong et al. 1992) to acquire echo-planar functional MR images (TR = 2 s, TE = 30 ms, flip angle = 70°, 64 × 64 image matrix, 3 × 3 mm in-plane resolution, 30 slices, 2.5 mm slice thickness with no gap, and ascending excitation order) in the AC–PC plane. Images were acquired starting from the superior convexity and extended ventrally so as to include the whole cerebral cortex, excluding only the ventral portion of the cerebellum. For each participant, we also acquired a three-dimensional high-resolution anatomical image (Siemens MPRAGE sequence, TR = 2 s, TE = 4.38 ms, flip angle = 8°, 512 × 512 image matrix, 0.5 × 0.5 mm in-plane resolution, and 176 contiguous 1 mm-thick sagittal slices). For each scan, we discarded the first four volumes to achieve

steady state, and the experimental task was initiated at the beginning of the fifth volume.

In separate days, each subject completed two 256 s-long visual motion scans and two or three 402 s-long scans of the Pointing/Saccade task and one anatomical scan. During the Pointing/Saccade task, subjects’ movements were supported by a dedicated MRI-compatible setup allowing subjects to perform controlled leg/foot movements (see Pitzalis et al. 2019 for a detailed description). To minimize movements during the scans, subjects’ head was stabilized with foam padding and with a chin rest mounted inside the head coil.

## Image processing and analysis

Images were pre-processed and analyzed using SPM12 (Wellcome Department of Cognitive Neurology, London, UK) and FreeSurfer 5.1 (<http://surfer.nmr.mgh.harvard.edu/>).

We first analyzed structural images following the “recon-all” fully automated processing pipeline implemented in FreeSurfer 5.1. This procedure allows us to obtain a surface representation of each individual cortical hemisphere in a standard space after performing intensity correction, transformation to Talairach space, normalization, skull-stripping, subcortical and white-matter segmentation, surface tessellation, surface refinement, surface inflation, sulcus-based nonlinear morphing to a cross-subject spherical coordinate system, and cortical parcellation (Dale et al. 1999; Desikan et al. 2006; Fischl et al. 1999a, b). The resulting surface reconstructions were transformed to the symmetrical FS-LR space (Van Essen et al. 2012) using tools in the Connectome Workbench software (<https://www.humanconnectome.org/software/get-connectome-workbench>), resulting in surface meshes with approximately 74 K nodes per hemisphere.

Functional images were realigned within and across scans to correct for head movement and coregistered with structural MPRAGE scans using SPM12 (Wellcome Department of Cognitive Neurology, London, UK). The functional data were then resampled to the individual cortical surface using ribbon-constrained resampling as implemented in Connectome Workbench (Glasser et al. 2013), and finally smoothed along the surface with an iterative procedure emulating a Gaussian kernel with a 6 mm Full Width at Half-Maximum (FWHM).

Functional images were then analyzed for each participant separately on a vertex-by-vertex basis, according to the General Linear Model (GLM). Separate regressors were included for each combination of effector (eye, hand, and foot), yielding parameter estimates for the average hemodynamic response evoked by each trial type. We modeled the whole-time interval from the target presentation to the end of the trial. We did not explicitly model blocks of fixation as GLM regressors, which were rather treated as part



of the residual variance. To reduce motion-induced noise, Framewise Displacement values (FD, Power et al. 2012), indicating the amount (in mm) of head movement relative to the previous time point, were also included in the model as nuisance regressors.

The analyses were conducted on six independently defined, theoretically motivated, Regions of Interest (ROIs; see below). These ROIs were defined only on the left hemisphere to account for the fact that participants used their right limb effector during the main experiment (Pointing/Saccade task). For each participant and region, we computed a regional estimate of the amplitude of the hemodynamic response, obtained by entering a spatial average (weighted for the most activated nodes within the region) of the pre-processed time series into the individual GLMs. Regional hemodynamic responses were thus analyzed through a series of one-sample *t* tests, assessing for each condition the presence of a reliable activation. This step was essential to establish which effector(s) the region was sensitive to. We applied a Bonferroni correction for multiple comparisons ( $p = 0.05/N = 3$ , i.e., the number of conditions). As a second step, to highlight any possible difference among conditions, we analyzed the BOLD signal change as a function of the experimental conditions by means of repeated-measure ANOVAs. The Shapiro–Wilk test indicated that all these variables were normally distributed ( $p > 0.05$ ). For these analyses, post hoc comparisons were computed after finding significant main effects and/or interactions, as paired *T* tests with Bonferroni correction for multiple comparisons.

### Gradient sensitivity ratio

In the six ROIs, the specificity of the BOLD responses to each of the three effectors was quantified by computing a sensitivity ratio between the BOLD signal for one effector and the sum of the BOLD signals for the three effectors (eye, hand, and foot). For example, the gradient sensitivity ratio of the eye condition was calculated as “eye/(eye + hand + foot)”. Results on the gradient sensitivity ratio computed in each ROI for each effector are visualized by coloring the parts of a ring shown on the flattened maps in Fig. 2A.

To complement the regional analysis, we assessed the effective connectivity among the above-mentioned regions using PPI analysis. This approach was used to examine how brain regions interact in a task-dependent manner (McLaren et al. 2012) by modeling BOLD responses in one target brain region in terms of the interaction between a psychological process and the neural signal from a source region. In other words, PPI allows testing whether experimental conditions (i.e., saccades, hand-, and foot pointing) modulate the functional connectivity between a source and a target region. For each participant and for all possible source-to-target

combinations, we modeled the BOLD signal in the target region as a combination of (a) the effects of the experimental conditions (saccades, hand pointing, and foot pointing), modeled through canonical hemodynamic functions, (b) a regressor containing the BOLD time course of the source region, which modeled the intrinsic functional connectivity between the source and the target region, and (c) two additional regressors expressing the interaction between trial-induced activation in each of the three conditions and the neural signal in the source region (PPI terms). PPI terms were built according to McLaren et al. (2012). Notice that PPIs effects modeling effective connectivity are built so as to be orthogonal to regressors modeling task-related activity. The resulting parameter estimates are expressed as percent signal changes in BOLD signal in the target region as a function of percent signal change in the seed region. We explored connectivity, separately for eye, hand, and foot trials, for all possible combinations of target and seed regions, by means of one-sample *t* tests, applying Bonferroni correction for multiple comparisons ( $p = 0.05/N = 30$ , i.e., number of sources regions  $\times$  number of target regions).

### Regions of interest (ROIs)

We focused our analyses on six egomotion regions (pIPS/V3A, V6+, IPSmot/VIP, pCi, CSv, and PIC) defined using the visual motion task. To localize areas preferentially responsive to coherent optic flow, we compared the BOLD response to coherently versus randomly moving dots. As originally described in Serra et al. (2019) and later also in other more recent papers from our lab (Di Marco, et al. 2021a, b; Sulpizio et al. 2020), this stimulus allows to define six distinct cortical regions strongly and bilaterally responsive to egomotion-compatible stimuli. As detailed in Serra et al. (2019), the six regions were anatomically located as follows (Fig. 2A): (1) the ventral portion of the posterior IntraParietal Sulcus (pIPS), mainly including the dorsal portion of the retinotopically defined V3A (Pitzalis et al. 2010; Sereno et al. 2001), that we call pIPS/V3A; (2) the V6 complex (or V6+) in the dorsal part of the Parieto-Occipital Sulcus (POS), including areas V6 and, anteriorly, V6Av, which was found to respond to this visual motion task, as well (Pitzalis, et al. 2013a, b; Tosoni et al. 2015); (3) the intraparietal motion area, known as IPSmot (Pitzalis et al. 2013a, b), in the horizontal segment of the IntraParietal Sulcus (IPS), likely corresponding to the human VIP (see Huang and Sereno, 2018) for a recent review), that we call IPSmot/VIP; (4) the posterior Cingulate sulcus area (pCi), within the posterior dorsal tip of the cingulate sulcus (Serra et al. 2019), corresponding to the precuneus motion area (Pc) originally described by Cardin and Smith (2010); (5) the Cingulate Sulcus visual area (CSv), in the depth of the posterior part of the cingulate sulcus, anterior to the posterior

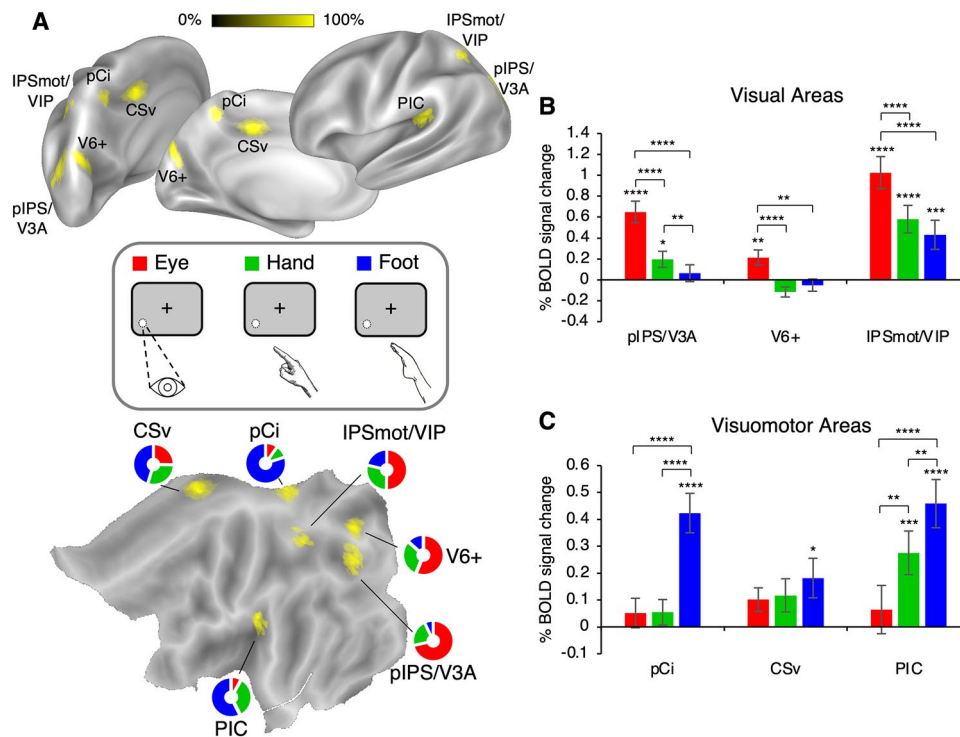


**Fig. 2** Region sensitivity to saccadic and hand/foot pointing movements. **A** Group overlap of the six individually defined egomotion-related ROIs rendered on the flattened and inflated (dorsomedial, medial, and lateral views) representation of the left hemisphere of the Conte69 surface-based atlas. Each yellow patch represents the weighted average location of individual ROIs. The color bar shows the level of saturation, where solid yellow represents the maximum overlap across 90% of total subjects. In the flat map, each colored ring visualizes the distribution of regional hemodynamic responses for the eye (red), hand (green), and foot (blue) conditions in the respective ROI. In inset of Fig. 2A, raw sketches describe the effector used and an example of the movement trajectory. Note that target

positions in the raw sketches were shown for display purpose only, since movements were performed only during the ‘go phase’ with respect to a ‘remembered’ target location not present anymore on the screen (see Fig. 1B). On the right, the plot shows the average of BOLD signal changes ( $\pm$ SE) in each ROI considered **B** visual and **C** visuomotor areas for eye, hand, and foot conditions relative to the fixation baseline. Asterisks above the columns refer to the *t* test versus zero. \* $p < .017$ , Bonferroni correction; \*\* $p < .01$ ; \*\*\* $p < .005$ ; \*\*\*\* $p < .001$ . Asterisks above square brackets refer to paired comparisons used to explore effector-related differences. \*\* $p < .01$ ; \*\*\*\* $p < .001$

ascending portion of the cingulate sulcus, corresponding to the original motion area described by Wall and Smith (2008); (6) the Posterior Insular Cortex (PIC), at the junction between the posterior insula and the PPC (see Greenlee et al. 2016 for a review). As observed in a previous study (Serra et al. 2019), the Flow Field stimulus also activates the lateral occipitotemporal MT complex (MT+), although less consistently. Nevertheless, this region, and in particular area MST, is considered one of the most prominent motion-sensitive regions in the macaque literature (for a review, see Orban 2008). However, in the lack of a functional localizer able to individually map this region in a consistent way, we cannot test this motion selective region. Future studies are required to establish the involvement of area MST in goal-directed movements.

In the results section, these six egomotion areas will be grouped into visual (pIPS/V3A, V6+, IPSmot/VIP

and visuomotor (pCi, CSv, PIC) areas. The rationale for this choice is based on recent results from our lab. Serra et al. (2019) observed that among the visual motion regions which are sensitive to egomotion-compatible visual stimuli, three areas (CSv, pCi, and PIC) responded also to long-range leg movements, whereas three areas (V6+, V3A, and IPSmot/VIP) do not. The authors hypothesized that whereas V6+, V3A, and IPSmot/VIP are likely involved only in the visual analysis of the optic flow (‘visual role’ and thus called ‘visual areas’), CSv, pCi, and PIC perform the visual analysis of egomotion-like signals to provide sensory information to the motor system with the aim of guiding locomotion (‘motor role’ and thus called ‘visuomotor areas’).

All the above-mentioned ROIs were defined on the surface cortical reconstruction as automatically obtained by FreeSurfer software package.

## Results

### Effector sensitivity of egomotion-related regions

As a first step, we used the visual motion task to define six egomotion-related visual areas (pIPS/V3A, V6+, IPSmot/VIP, pCi, CSv, and PIC) as recently described in Serra et al. (2019). Figure 2A shows the average location of these six regions, projected onto an inflated and a flattened representation of a standard brain. The same inflated hemisphere is shown in multiple views (lateral, medial, and dorsomedial). Only the left hemisphere of each brain is shown, since participants used their right limb as effector during the Pointing/Saccade task.

We then studied the functional response profile of the six areas during the Pointing/Saccade task to explore their sensitivity to goal-directed pointing movements performed by different effectors. The mean percent signal change observed in each of these regions for the three effectors (eye, hand, and foot) is plotted in the column histograms of Fig. 2B, C. Based on Serra et al. (2019); see method for details, results are separately rendered and described for the visual (Fig. 2B) and visuomotor (Fig. 2C) sets of ROIs. To reveal regions with a significant positive response to any saccade/pointing movements, we used one-sample *t* tests versus zero.

As to the visual regions, plots in Fig. 2B reveal that all three areas responded to eye condition (pIPS/V3A,  $t_{13} = 6.26$ ,  $p = 1.47 \times 10^{-5}$ ; V6+,  $t_{15} = 2.93$ ,  $p = 5.16 \times 10^{-3}$ ; IPSmot/VIP,  $t_{15} = 6.67$ ,  $p = 3.73 \times 10^{-6}$ ). However, while V6+ showed no significant or negative responses to the other effectors (hand pointing,  $t_{15} = 2.42$ ,  $p = 0.014$ ; foot pointing,  $t_{15} = 0.87$ ,  $p = 0.198$ ), pIPS/V3A responded also to hand pointing ( $t_{13} = 2.55$ ,  $p = 0.012$ ) but not to foot pointing ( $t_{13} = 0.79$ ,  $p = 0.221$ ), and IPSmot/VIP responded also to the other two effectors (hand pointing,  $t_{15} = 4.41$ ,  $p = 2.54 \times 10^{-4}$ ; foot pointing,  $t_{15} = 3.10$ ,  $p = 3.66 \times 10^{-3}$ ).

As to the visuomotor regions, plots in Fig. 2C reveal that all the three areas showed a significant positive response to foot pointing (pCi,  $t_{13} = 5.76$ ,  $p = 3.28 \times 10^{-5}$ ; CSv,  $t_{14} = 2.47$ ,  $p = 0.013$ ; PIC,  $t_{14} = 5.11$ ,  $p = 7.93 \times 10^{-5}$ ). Only PIC responded to hand pointing ( $t_{14} = 3.40$ ,  $p = 2.18 \times 10^{-3}$ ), while the other two regions did not (pCi,  $t_{13} = 1.14$ ,  $p = 0.137$ ; CSv,  $t_{14} = 1.90$ ,  $p = 0.039$ ). None of the three visuomotor areas showed a response to the eye condition (pCi,  $t_{13} = 0.94$ ,  $p = 0.182$ ; CSv,  $t_{14} = 2.31$ ,  $p = 0.018$ ; PIC,  $t_{14} = 0.72$ ,  $p = 0.242$ ).

To reveal any significant effector-related differences, the BOLD percent signal change underwent a one-way repeated-measures ANOVA with effector as factor (eye, hand, and foot).

As to the visual regions (see plots in Fig. 2B), the ANOVA showed a main effect of effector in all the

three areas. In area V3A, the main effect ( $F_{2,26} = 47.49$ ,  $p < 0.001$ ,  $\eta_p^2 = 0.785$ ) indicated a stronger response during saccade as compared to both hand and foot pointing (eye > hand,  $p < 0.001$ ; eye > foot,  $p < 0.001$ ) as well as a significant difference between hand and foot (hand > foot,  $p = 0.015$ ). In both areas V6+ and IPSmot/VIP, the significant main effect of effector (V6+:  $F_{2,30} = 14.85$ ,  $p < 0.001$ ,  $\eta_p^2 = 0.498$ ; IPSmot/VIP:  $F_{2,30} = 18.92$ ,  $p < 0.001$ ,  $\eta_p^2 = 0.558$ ) indicated that the BOLD response was significantly higher during saccade with respect to both hand and foot pointing (V6+: eye > hand,  $p = 0.012$ ; eye > foot,  $p < 0.001$ ; IPSmot/VIP: eye > hand,  $p = 0.001$ ; eye > foot,  $p < 0.001$ ), which did not differ against each other (V6+:  $p = 0.732$ ; IPSmot/VIP:  $p = 0.242$ ).

As to the visuomotor regions (see plots in Fig. 2C), the ANOVA showed a main effect of effector in all the three areas, except in area CSv. In area pCi, the main effect ( $F_{2,26} = 15.33$ ,  $p < 0.001$ ,  $\eta_p^2 = 0.541$ ) indicated a stronger response in foot with respect to hand and eye (foot > hand,  $p < 0.001$ ; foot > eye,  $p = 0.007$ ) which did not differ against each other ( $p = 0.999$ ). In area PIC, the main effect ( $F_{2,28} = 15.83$ ,  $p < 0.001$ ,  $\eta_p^2 = 0.531$ ) indicated a stronger response in foot as compared to both hand and eye (foot > hand,  $p = 0.016$ ; foot > eye,  $p = 0.001$ ) as well as a significant difference between hand and eye (hand > eye,  $p = 0.015$ ).

To better visualize the differential effector sensitivity for each region, we computed the relative size of the BOLD signal for saccades, and hand and foot pointing by weighting the activity evoked by each condition with respect to that evoked by the sum of all conditions (Fig. 2A), and color coded the resulting circles rendered on the flat maps according to the effector preference observed in each area. This color coding clearly illustrates the different trends observed in the two sets of regions. Indeed, as revealed by the gradient sensitivity ratio in Fig. 2A, while in the visual regions, the BOLD response is mainly driven by the eye condition (red), in the visuomotor regions, the BOLD response is mainly driven by the foot condition (blue).

To sum up, we observed a postero-anterior gradient of preference for eye-to-foot movements. Only the most caudal egomotion areas preferred saccades, whereas only the most rostral egomotion areas preferred foot pointing. In contrast, we did not observe in any area a clear preference for hand pointing, which seems more uniformly distributed across the six egomotion regions.

### Seed-to-seed connectivity of egomotion-related regions

To assess whether regions with a different functional profile also show a different coupling as a function of the specific effector used in the Pointing/Saccade task, we conducted

an effective connectivity analysis using a generalized form of PsychoPhysiological Interaction analysis (gPPI). This analysis could shed some light on the functional differences and similarities between regions we found from the previous analyses.

Tables 2, 3, 4 show all PPIs (namely, effective connectivity during different experimental conditions) for each possible pair of source and target regions, separately for each condition (eye condition: Table 2, hand condition: Table 3, foot condition: Table 4). To assess the presence of significant coupling among the six identified egomotion areas during eye/hand/foot movements, we used one-sample t test versus zero for each pair of ROIs.

The Bonferroni-corrected results of the seed-to-seed connectivity analysis are also graphically represented in

Fig. 3 separately for eye (A, red arrows), hand (B, green arrows), and foot (C, blue arrows) conditions. In each panel, the color-coded arrows indicate the direction of effective connectivity among the two sets of visual (left: pIPS/V3A, V6+ and IPSmot/VIP) and visuomotor (right: pCi, CSv and PIC) areas.

In the eye saccade condition (Table 2, Fig. 3A), all the three visual areas were connected with CSv (pIPS/V3A,  $t_{11} = 5.22, p = 1.44 \times 10^{-4}$ ; V6+,  $t_{14} = 7.90, p = 7.98 \times 10^{-7}$ ; IPSmot/VIP,  $t_{13} = 3.70, p = 1.32 \times 10^{-3}$ ). In addition, both pIPS/V3A and IPSmot/VIP showed significant connections with the other visual areas. More specifically, pIPS/V3A was connected with both V6+ ( $t_{12} = 5.54, p = 6.35 \times 10^{-5}$ ) and IPSmot/VIP ( $t_{12} = 5.38, p = 8.31 \times 10^{-5}$ ), and IPSmot/VIP was connected with both pIPS/V3A ( $t_{12} = 6.16,$

**Table 2** Effective connectivity results for the eye saccade condition

	Target					
	Visual areas			Visuomotor areas		
	pIPS/V3A	V6+	IPSmot/VIP	pCi	CSv	PIC
<b>Source</b>						
<b>Visual areas</b>						
pIPS/V3A		<b><math>6.35 \times 10^{-5}</math>***</b>	<b><math>8.31 \times 10^{-5}</math>***</b>	<b><math>1.2 \times 10^{-4}</math>**</b>	<b><math>1.44 \times 10^{-4}</math>***</b>	+
V6+	+		+	+	<b><math>7.98 \times 10^{-7}</math>****</b>	<b><math>3.86 \times 10^{-4}</math>**</b>
IPSmot/VIP	<b><math>2.44 \times 10^{-5}</math>***</b>	<b><math>1.09 \times 10^{-3}</math>*</b>		+	<b><math>1.32 \times 10^{-3}</math>*</b>	n.s
<b>Visuomotor areas</b>						
pCi	<b><math>7.37 \times 10^{-5}</math>***</b>	+	+		+	+
CSv	n.s	+	+	+		+
PIC	n.s	+	n.s	n.s	+	

No significant t test versus 0 is coded n.s. Asterisks refer to t test versus zero. +  $p < .05$ , Bonferroni uncorrected  $p < .0017$ , Bonferroni correction; \*\* $p < .0001$ ; \*\*\* $p < .00001$ ; \*\*\*\* $p < .000001$ . Significant and Bonferroni-corrected data are shown in bold

**Table 3** Effective connectivity results for the hand pointing condition

	Target					
	Visual areas			Visuomotor areas		
	pIPS/V3A	V6+	IPSmot/VIP	pCi	CSv	PIC
<b>Source</b>						
<b>Visual areas</b>						
pIPS/V3A		<b><math>3.13 \times 10^{-4}</math>**</b>	+	<b><math>4.92 \times 10^{-4}</math>**</b>	+	<b><math>8.59 \times 10^{-4}</math>**</b>
V6+	+		n.s	+	+	<b><math>2.00 \times 10^{-5}</math>***</b>
IPSmot/VIP	<b><math>1.21 \times 10^{-4}</math>**</b>	+		+	+	<b><math>2.47 \times 10^{-4}</math>**</b>
<b>Visuomotor areas</b>						
pCi	+	+	n.s		<b><math>1.54 \times 10^{-3}</math>*</b>	+
CSv	n.s	+	+	n.s		<b><math>6.92 \times 10^{-4}</math>**</b>
PIC	n.s	<b><math>7.80 \times 10^{-4}</math>**</b>	+	+	+	

No significant t test versus 0 is coded n.s. Asterisks refer to t test versus zero. +  $p < .05$ , Bonferroni uncorrected

\* $p < .0017$ , Bonferroni correction; \*\* $p < .0001$ ; \*\*\* $p < .00001$ . Significant and Bonferroni-corrected data are shown in bold



**Table 4** Effective connectivity results for the foot pointing condition

	Target					
	Visual areas			Visuomotor areas		
	pIPS/V3A	V6+	IPSmot/VIP	pCi	CSv	PIC
Source						
Visual areas						
pIPS/V3A		<b><math>8.05 \times 10^{-4}</math>**</b>	+	+	+	n.s
V6+	n.s		n.s	+	+	<b><math>1.10 \times 10^{-3}</math>**</b>
IPSmot/VIP	+	n.s		+	<b><math>2.42 \times 10^{-4}</math>**</b>	+
Visuomotor areas						
pCi	n.s	+	<b><math>6.37 \times 10^{-5}</math>***</b>		<b><math>4.51 \times 10^{-4}</math>**</b>	+
CSv	n.s	+	+	+		<b><math>9.62 \times 10^{-4}</math>**</b>
PIC	n.s	<b><math>8.15 \times 10^{-4}</math>**</b>	n.s	+	+	

No significant *t* test versus 0 is coded n.s. Asterisks refer to *t* test versus zero. +*p* < .05, Bonferroni uncorrected

\**p* < .0017, Bonferroni correction; \*\**p* < .0001; \*\*\**p* < .00001. Significant and Bonferroni-corrected data are shown in bold

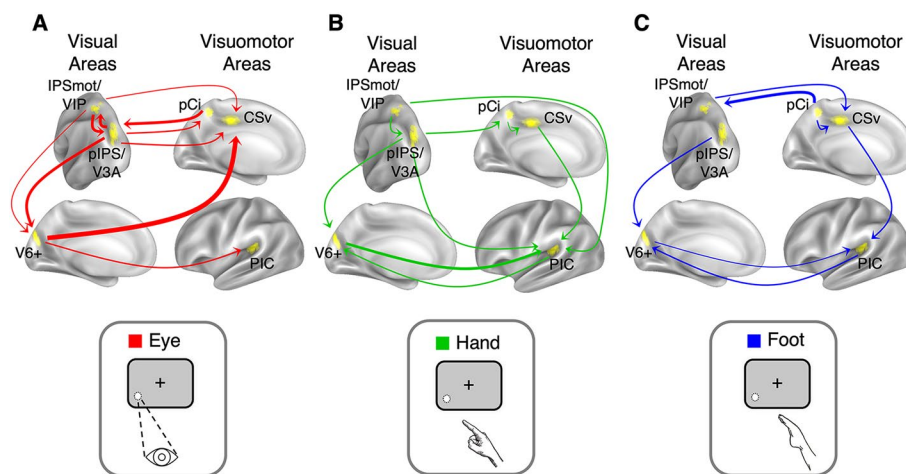


**Fig. 3** PPIs seed-to-seed. PPIs showing significant effects are schematically represented by directional arrows. Arrows identify source-to-target directions for each experimental condition: **A** eye condition with red arrows, **B** hand condition with green arrows, and **C** foot condition with blue arrows. In inset, raw sketches describe the effector used and an example of the movement trajectory. Different arrow line thicknesses represent the statistical significance of each connection.

$p = 2.44 \times 10^{-5}$ ) and V6+ ( $t_{14} = 3.75$ ,  $p = 1.09 \times 10^{-3}$ ). Other connections starting from a visual area and targeting a visuomotor area were pIPS/V3A vs. pCi ( $t_{10} = 5.56$ ,  $p = 1.20 \times 10^{-4}$ ), and V6+ vs. PIC ( $t_{13} = 4.36$ ,  $p = 3.86 \times 10^{-4}$ ). Finally, area pCi was the only visuomotor area showing significant effective connectivity during the eye condition. This area indeed showed a significant coupling with pIPS/V3A ( $t_{10} = 5.92$ ,  $p = 7.37 \times 10^{-5}$ ). Reciprocal connections were found between pIPS/V3A and IPSmot/VIP as well as between pIPS/V3A and pCi. Overall, during the eye movements, we observed a total number of ten significant

connections: nine (9/10; 90%) started from the visual areas (4 from pIPS/V3A, 3 from IPSmot/VIP, and 2 from V6+) and only one (1/10; 10%) from the motor areas (1 from pCi). During the hand pointing condition (Table 3, Fig. 3B), all the three visual areas and the visuomotor area CSv were connected with PIC (pIPS/V3A,  $t_{12} = 4.01$ ,  $p = 8.59 \times 10^{-4}$ ; V6+,  $t_{13} = 6.07$ ,  $p = 2.00 \times 10^{-5}$ ; IPSmot/VIP,  $t_{13} = 4.60$ ,  $p = 2.47 \times 10^{-4}$ ; CSv,  $t_{12} = 4.13$ ,  $p = 6.92 \times 10^{-4}$ ). Significant couplings were observed between pIPS/V3A and pCi ( $t_{10} = 4.60$ ,  $p = 4.92 \times 10^{-4}$ ), IPSmot/VIP and pIPS/V3A ( $t_{12} = 5.15$ ,  $p = 1.21 \times 10^{-4}$ ), and pCi and CSv ( $t_{11} = 3.77$ ,

$p = 1.54 \times 10^{-3}$ ). Area V6+ was the target of significant couplings starting from both pIPS/V3A ( $t_{12} = 4.59$ ,  $p = 3.13 \times 10^{-4}$ ) and PIC ( $t_{13} = 3.98$ ,  $p = 7.80 \times 10^{-4}$ ). Reciprocal connections were found only between V6+ and PIC. Overall, during the hand pointing movements, we observed a total number of nine significant connections: six (6/9; 67%) started from the visual areas (3 from pIPS/V3A, 2 from IPSmot/VIP and 1 from V6+) and three (3/9; 33%) from the motor areas (1 from pCi, 1 from CSv and 1 from PIC).

During the foot pointing condition (Table 4, Fig. 3C), the only connections starting from the visual areas were: pIPS/V3A vs. V6+ ( $t_{12} = 4.05$ ,  $p = 8.05 \times 10^{-4}$ ), V6+ vs. PIC ( $t_{13} = 3.80$ ,  $p = 1.10 \times 10^{-3}$ ), and IPSmot/VIP vs. CSv ( $t_{13} = 4.61$ ,  $p = 2.42 \times 10^{-4}$ ). pCi was the only area showing at least two significant connections, targeting both IPSmot/VIP ( $t_{12} = 5.54$ ,  $p = 6.37 \times 10^{-5}$ ) and CSv ( $t_{11} = 4.50$ ,  $p = 4.51 \times 10^{-4}$ ). The remaining visuomotor areas, CSv and PIC, were connected, respectively, with PIC ( $t_{12} = 3.95$ ,  $p = 9.62 \times 10^{-4}$ ) and V6+ ( $t_{13} = 3.96$ ,  $p = 8.15 \times 10^{-4}$ ). Like for hand pointing, reciprocal connections were found only between V6+ and PIC. Overall, during the foot pointing movements, we observed a total number of seven significant connections: four (4/7; 57%) started from the visuomotor areas (2 from pCi, 1 from CSv and 1 from PIC) and three (3/7; 43%) from the visual areas (1 from pIPS/V3A, 1 from V6+ and 1 from IPSmot/VIP).

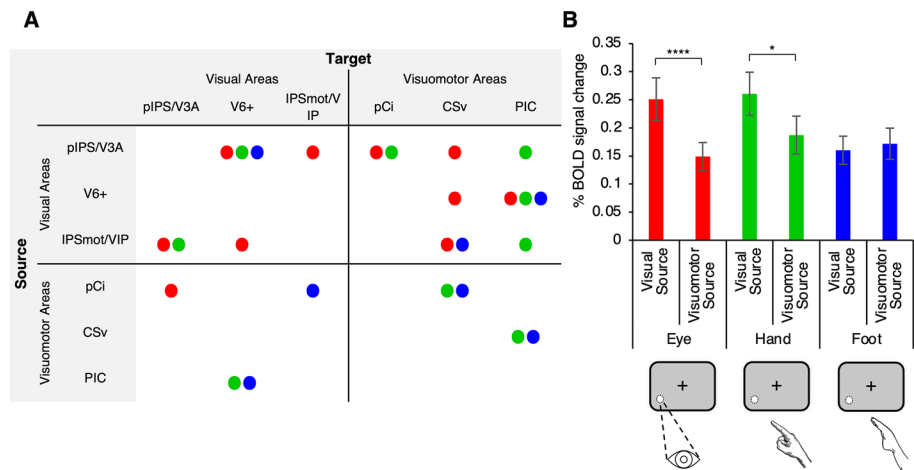
All the significant Bonferroni-corrected seed-to-seed PPIs described above are resumed in Fig. 4A, where the connections between regions are combined and color coded depending on the effector used. A first observation is that the number of connections starting from the visual and the visuomotor source regions appeared different as a function of the specific effector used in the Pointing/Saccade task. Specifically, the total number of connections starting from the visual areas was maximum during saccades (9/18; 50%) and progressively decreased during hand (6/18; 33%) and foot (3/18; 17%) pointing. In

contrast, the total number of connections starting from the visuomotor areas was maximal during foot pointing (4/8; 50%), and progressively decreased during hand (3/8; 38%) and eye (1/8; 13%) movements.

To substantiate these observations, we performed a formal comparison between the regions and the effectors. Since we were interested in revealing different functional connections between visual and visuomotor egomotion regions, we collapsed together results from the visual and the visuomotor regions and analyzed their effective connectivity through a source (visual, visuomotor) by target (visual, visuomotor) by effector (foot, hand, eye) repeated-measure ANOVA. The reported results are corrected for multiple comparisons using the Bonferroni method (see the Materials and methods section).

The ANOVA showed a significant interaction between source and target ( $F_{1,16} = 8.23$ ,  $p = 0.011$ ,  $\eta_p^2 = 0.340$ ), indicating that the connections received by the visual regions originate more from visual than visuomotor regions ( $p = 4.87 \times 10^{-3}$ ). This suggests that the visual regions are more interconnected with each other with respect to the visuomotor regions. We also observed a significant interaction between effector and source ( $F_{2,32} = 12.48$ ,  $p = 9.83 \times 10^{-5}$ ,  $\eta_p^2 = 0.588$ ; see Fig. 4B) indicating a greater connectivity that originates from the visual regions compared to the visuomotor ones, in particular during both eye ( $p = 3.85 \times 10^{-4}$ ) and hand ( $p = 0.042$ ) movements. No significant effect of the source regions was instead observed during foot pointing movements. Although the trend is reversed with slightly larger connections starting from the visuomotor rather than visual regions, this difference did not reach statistical significance ( $p = 1.00$ ). Overall, the main results of the PPI analyses can be summarized as follows. First, the visual regions are more interconnected to each other with respect to the visuomotor regions. Second, the connections starting from the visual and the visuomotor sources regions were different in terms of numerosity and greatness as a function

**Fig. 4** **A** The table resumes significant seed-to-seed PPIs. ● = Eye saccade; ● = Hand pointing; ● = Foot pointing. **B** The plot shows the average of BOLD signal changes ( $\pm$  SE) as a function of effector (eye, hand, and foot) and source (visual and visuomotor). In inset of Fig. 4B, raw sketches describe the effector used and an example of the movement trajectory. Asterisks above square brackets refer to Bonferroni-corrected post hoc tests. \* $p < .05$ ; \*\*\* $p < .001$



of the specific effectors used in the Pointing/Saccade task, particularly during eye and hand movements.

A second observation from Fig. 4A is that, beyond the presence of some specific regions showing a connectivity pattern reflecting some degree of effector specificity, we also observed that the effective connectivity of other regions was effector independent. Indeed, both connections starting from pIPS/V3A and targeting V6+, and those starting from V6+ and targeting PIC, were present in all three conditions (and are the only ones marked in Fig. 4A with three dots).

## Discussion

In the present study, we used a combined approach of task-evoked activity and effective connectivity (PPI) analysis to reveal whether visual (pIPS/V3A, V6+, IPSmot/VIP) and visuomotor (pCi, CSv, PIC) cortical areas involved in processing optic flow signals are also differentially sensitive to goal-directed pointing movements performed with different effectors (eyes, hand, and foot). This allowed us to suggest the possible differential functional roles played by visual and visuomotor regions in self-motion signal processing.

Hereafter, regions will be grouped by their different functional profiles and discussed considering previous evidence from macaque and human brain studies. We will use the terms selectivity and preference to refer, respectively, to cortical regions responding only to one effector or to more than one effector with a preference for one of them, respectively. However, it should be noted that the concept of selectivity has here a limited validity as it is based on the comparison of just three task settings.

### Effector preference in visual (pIPS/V3A, V6+, IPSmot/VIP) and visuomotor (pCi, CSv, PIC) egomotion regions

A first result of this study is that we found a clear preference for saccades in all three visual egomotion areas, pIPS/V3A, V6+, and IPSmot/VIP.

The three visual egomotion areas exhibited different functional profiles with respect to the other two effectors. Area V6+ was the only one showing no significant responses to hand and foot pointing movements, and thus, it can be considered *selective* for the eye movements. The response to goal-directed pointing movements in area V6+ was also tested in a few previous studies, where we observed an almost null or weak response to hand pointing (Pitzalis et al. 2013a, b), as found in the present study, and greater BOLD responses to the execution of eye movements relative to pointing movements (Tosoni et al. 2015). Area IPSmot/VIP was the only one of the three visual egomotion areas showing significant responses also to the other two

effectors besides the eye, with comparable BOLD signals in hand and foot pointing (although weaker with respect to saccades). This implies that area IPSmot/VIP is activated by the pointing action regardless of the limb used (upper or lower). This result is in line with the historical failure to find effector specificity in the PPC. Indeed, previous studies (Heed et al. 2011; Leone et al. 2014; Pitzalis et al. 2019) revealed a shared neural substrate in the PPC for hand and foot pointing, possibly confirming a functional—rather than an effector—specificity within the posterior intraparietal sulcus. We can conclude that in these visual areas, we found a null response to foot pointing or, if any, comparable to that observed for hand pointing.

A second result of this study is that, unlike the visual areas, the visuomotor regions pCi and PIC showed a preference for foot pointing movements as compared to the other effectors, and area CSv showed a reliable activation only during foot pointing movements.

While several neurophysiological and neuroimaging studies have compared eye and hand movements to demonstrate that distinct neural circuits are preferentially active for movements involving different body parts (Andersen and Cui, 2009; Caminiti et al. 2010; Galati et al. 2011; Graziano and Gross 1998; Tosoni et al. 2015), only a few fMRI studies (Heed et al. 2011, 2016; Leone et al. 2014; Maltempo et al. 2021; Medendorp and Heed 2019; Pitzalis et al. 2019) have tested also movements involving the lower limbs, comparing activity during memory guided eye, hand, and foot movements. The whole-brain maps showed in the early studies revealed a lateral-to-medial hand-foot organization (Heed et al. 2011; Huang et al. 2012; Leone et al. 2014; Pitzalis et al. 2019). Indeed, the network of areas involved in foot pointing control was found mainly located on the medial wall, including the medial portion of M-I and S-I, and extending posteriorly up to the cingulate sulcus. However, these studies revealed that this foot pointing network does not include only medial regions (including the three leg-related sensorimotor regions hPEc, hPE, and S-I), but it is more distributed throughout the brain including also portion of the lateral wall. In Pitzalis et al. (2019), we further characterized the activation on the lateral wall, since foot-related activation was also found in the posterior portion of the insular cortex (where PIC is located). Area PIC in the Sylvian fissure is a motion region responding to visual and vestibular motion stimulation, presumably supporting the integration of motion information from visual and vestibular senses for the perception of self-motion (Frank et al. 2016a, b; Frank et al. 2016a, b; Frank and Greenlee 2018). While the optic flow sensitivity in this region is known in both human (Cardin and Smith 2010; Serra et al. 2019) and macaque brain (Cottareau et al. 2017; Pitzalis et al. 2021), the response to both foot and hand pointing observed here in area PIC is a new result and is in line with the suggested

involvement of this region in whole-body actions requiring both upper and lower limb movements. It has recently been suggested that area PIC plays a crucial role in somatosensory discrimination during active touch and haptic exploration, demonstrating a greater sensitivity of this area to touch during self-generated movement compared to that induced by functional electrical stimulation (Limanowski et al. 2019). In agreement with previous studies (Heed et al. 2011; Leone et al. 2014), we found that a true limb (hand/foot) preference does not involve posterior medial and lateral parietal and occipital regions (where the three visual egomotion regions pIPS/V3A, V6+ and IPSmot/VIP are located).

Overall, we observed a differentiated functional profile among the six egomotion areas, namely a postero-anterior gradient of preference for eye-to-foot movements. Only the most caudal visual areas were preferentially activated during saccades, whereas only the most rostral visuomotor areas responded preferentially to foot pointing. In contrast, none of the tested regions showed a preference for hand pointing movements. The lack of a gradient of preference for hand pointing is not completely surprising. Previous studies (Filimon et al. 2009; Hagler et al. 2007), indeed, have provided similar results, leading to the hypothesis that hand pointing movements, being short-range limb actions, are likely not able to maximally activate the somatomotor cells of the dorsal parietal regions (where the arm is represented) and to activate reach-related areas more than saccades (Filimon 2010). Note, however, that beside the lack of a cortical area with a specific preference for the hand condition, we observed a statistically significant response for hand pointing in three areas (pIPS/V3A, IPSmot/VIP, PIC). This means that these areas have a hand representation, although not preferred with respect to other effectors. This result is in line with the more general concept that during self-motion, we typically have to visually guide whole-body actions which involve movements performed by upper and lower limbs.

It is worth saying that whole-brain mapping analyses previously reported some degrees of effector preference in a wide network of cortical areas, including medial parietal areas where egomotion-related areas responding to optic flow are located (e.g., Heed et al. 2011). However, these analyses described such activations in terms of whole-brain neural circuits, not ascribed to specific brain regions. Using a regional approach, we aimed at testing and comparing, in a more direct way, the effector sensitivity of cortical regions responding to egomotion-compatible stimulation. Note also that while the response in occipito-parietal visual areas (pIPS/V3A, V6+, and IPSmot/VIP) to saccades and hand pointing was already partially documented, their response to foot pointing movements has never been tested before. By simultaneously testing the response of the three "visual" areas to the three effectors enables us to reveal that beside the preference to eye movements, there are visual areas, like

VIP, that respond to all the effectors while areas, like V6, that respond only to one effector. This is another novel piece of evidence that could not be predicted based on previous literature.

### **Effective connectivity between visual (pIPS/V3A, V6+, IPSmot/VIP) and visuomotor (pCi, CSv, PIC) egomotion regions**

We also performed an effective connectivity analysis to verify whether regions with a different functional profile also show a different coupling as a function of the specific effector used in the Pointing/Saccade task.

The pattern of functional cortical connections of pIPS/V3A, V6+, and IPSmot/VIP appears consistent with the saccade preference observed in the task-evoked analysis. Indeed, we found greater connectivity that originates from the visual regions compared to the visuomotor ones, especially during saccades and, to a lesser extent, also during hand pointing movements. Moreover, only during saccades, we found reciprocal connections between pIPS/V3A and IPSmot/VIP as well as between pIPS/V3A and pCi. Among these connections, only the former (VIP-V3A) was also confirmed by a previous resting-state functional connectivity study (fcMRI) (Serra et al. 2019), while the latter (pIPS/V3A-pCi) did not. Differences between present and previous results can be explained considering the different connectivity analyses used, and suggest that some connections are not evident at rest but emerge only when subjects are engaged in a pointing task using the preferred effector (eye).

The pattern of functional cortical connections of pCi, CSv, and PIC revealed that the visuomotor regions are less interconnected to each other with respect to the visual regions. Moreover, the connections starting from the visuomotor regions were uniformly distributed between visual and visuomotor regions. Interestingly, we found connections between pCi and CSv, as well as between CSv and PIC during both hand and foot pointing, but not during saccades. This implies that the connections between the visuomotor regions were captured better by movements performed by the lower and upper limbs, which are typically used to act on objects in the surrounding space, than by eye movements, which are instead typically used to explore the visual field. However, the pattern of functional cortical connections of pCi, CSv, and PIC revealed a less clear-cut profile in terms of effector preference. Indeed, although the number of connections originating from the visuomotor areas was the highest during foot pointing and gradually decreased during hand pointing to be almost absent during saccades, there were no significant statistical differences in the pattern of effective connectivity originating from all the visuomotor areas among the three conditions (see Fig. 4B).



Besides the presence of an effector-dependent pattern of connectivity among some of the studied regions, we also found evidence of effective connectivity which was effector independent in some other regions, such as pIPS/V3A vs V6+ as well as V6+ vs PIC. These connections were observed in all three conditions, and thus independently of the effector (eye, hand, or foot) used during the pointing movements. The presence of task-unrelated connections between these regions is in line with results from previous human fcMRI studies (Serra et al. 2019; Tosoni et al. 2015) where the connections between V6+ and the retinotopic V3A as well as the vestibular PIC were found also at rest (i.e., with no experimenter-imposed task and closed eyes). Previous and present results suggest that the connections between these regions are solid and consistently found independently of the effector and task performed. Although caution is needed in the interpretation of the functional connectivity data (Buckner et al. 2013; Smith et al. 2018), the connections of area V6+ with the dorsal visual area V3A found here strictly mirror the pattern of anatomical connections of the macaque area V6 (Galletti et al. 2001).

Overall, while the connectivity originating from the visual regions compared to the visuomotor ones was greater during saccades (supporting the eye preference observed in the task-evoked analysis) and, at lower extent, also during hand pointing movements, the connections observed in the visuomotor areas were not strong enough to support a clear foot pointing preference. The PPI analysis also revealed signs of either effector-dependent or effector-unrelated (or independent) functional cortical connections between the six egomotion regions.

### Differential functional role of the visual and visuomotor egomotion areas

Taken together, the above-described task-evoked and connectivity results suggest that visual (pIPS/V3A, V6+, IPSmot/VIP) and visuomotor (pCi, CSv, PIC) egomotion regions process self-motion signals for different purposes.

V3A, V6+, and VIP are retinotopically organized (Huang and Sereno 2007; Pitzalis et al. 2006; Tootell et al. 1997), respond to flow fields in both humans (Serra et al. 2019; Sulpizio et al. 2020) and macaques (Pitzalis et al. 2021), and to self-motion compatible visual stimulation (Cardin and Smith 2010; Pitzalis et al. 2020; Wall and Smith 2008). In addition, previous fMRI studies have shown that areas V3A, V6, and VIP respond to visual motion stimuli simulating continuous heading changes (Furlan et al. 2014; Huang et al. 2015) and steering (Di Marco et al. 2021a, b). These regions, however, do not respond to leg movements and are not directly connected to medial sensory and motor cortices where lower limbs are represented (Serra et al. 2019). As we have already pointed out, the three visual egomotion

regions (pIPS/V3A, V6+, IPSmot/VIP) have properties that constitute important prerequisites for a visual analysis of the retinal signals due to self-motion (Di Marco et al. 2021a, b; Serra et al. 2019; see for review Cheng and Gu 2018). In particular, we and others have proposed that these regions are involved in a visual process, known as flow parsing, that consists of the capability to subtract self-motion components from retinal motion signals with the aim of extracting object motion information (Field et al. 2020; Galletti and Fattori 2003, 2018; Pitzalis et al. 2015, 2020). The preference for saccades found here supports the involvement of these regions in ‘visual’ aspects of self-motion processing. Indeed, during self-motion, the upper and lower limbs are typically used to manipulate and interact with the environment, while the eyes are used to visually explore the environment by aligning the fovea with surrounding elements of interest to capture their visual features (size, shape, color, etc.). Thus, given the ‘visual’ role played by the eyes during self-motion, it is reasonable to assume that saccadic movements recruit cerebral regions that are located early in the visual cortical pathways and are retinotopically organized (Pitzalis et al. 2006; Sereno and Huang 2006; Tootell et al. 1997).

In recent years, we have witnessed a change in perspective and views on the three visuomotor egomotion regions (pCi, CSv, and PIC). At the beginning, many fMRI studies revealed that they share several visual properties with the visual egomotion areas pIPS/V3A, V6+, and IPSmot/VIP. Indeed, they respond to flow field visual stimulation (Aedo-Jury et al. 2020; Serra et al. 2019; Sulpizio et al. 2020), to self-motion compatible visual stimulation (Cardin and Smith 2010; Huang et al. 2015; Pitzalis et al. 2020), and to heading changes and self-motion direction estimation, especially during locomotion (Di Marco et al. 2021a, b). Note that a preference for optic flow was also found in the corresponding macaque regions, called in monkey, respectively, pmCSv (putative macaque CSv; Cottureau et al. 2017; but see Pitzalis et al. 2021) and VPS (Visual Posterior Sylvian region putatively homologue to the human PIC; Cottureau et al. 2017; Pitzalis et al. 2021).

Recently, it has been widely documented that the three visuomotor egomotion regions also play a *motor* role. pCi, CSv, and PIC not only respond to optic flow, but also to long-range leg movements (Serra et al. 2019) and are functionally connected with the medial part of somatosensory and motor areas (where legs and feet are represented). Recent evidence supports the hypothesis that some of these visuomotor regions play a role in multimodal self-motion integration (e.g., Di Marco et al. 2021a, b; Schindler and Bartels 2018). In a recent study (Di Marco et al. 2021a, b), in particular, we tested the responses of these three visuomotor egomotion regions in a multisensory integration experiment combining visual and somatomotor signals relevant to locomotion in congruent and



incongruent trials. Results revealed that pCi and PIC (but not CSv) showed sensitivity to congruency, suggesting that these two regions are able to integrate congruent visual and somatomotor signals relevant to locomotion. The preference for foot pointing movements observed in pCi and PIC is a new and significant result of the present study that further strengthens the possible involvement of these areas in the motor control of lower limb movements. Here, we found a selectivity foot pointing movement in the cingulate visuomotor areas pCi and CSv, and a preference for foot pointing in PIC which responds also to hand pointing movement. The selectivity/preference we observed here for foot pointing movements, combined with previous evidence of a multimodal integration of somatomotor signals and visual motion information in pCi and PIC (Di Marco et al. 2021a, b), supports the hypothesis that these regions are directly engaged in visually guided locomotion control by sending visual and somatomotor signals to the motor system. We suggest that PIC is likely activated also during walking in a dynamic environment to visually guide our lower and upper limb movements. These regions might be key interfaces between the sensory and motor systems in the context of the control of locomotion (see also Smith 2021 for a similar interpretation of area CSv).

Overall, the present results from both task-evoked and effective connectivity analyses, combined with previous results achieved in these areas over the years, support the hypothesis that visual and visuomotor egomotion regions likely perform different roles within a network aimed at subserving sensory–motor integration during our movement in the external environment. The most posterior regions, pIPS/V3A, V6+, and IPSmot/VIP, seem mainly involved in the visual analysis of the egomotion retinal components (and in the flow parsing mechanism) essential to coordinate eye and arm movements during exploration in a complex and dynamic environment. Conversely, the most anterior regions, pCi, CSv, and PIC, likely play a motor role in the processing of the egomotion signal, combining visual and somatomotor cues coming from the lower limbs, to allow a visually guided control of locomotion.

**Author contributions** All authors had full access to all the data in the study and take responsibility for the integrity of the data and the accuracy of the data analysis. Conceptualization: MB, VS, PF, CG, GG, TM, and SP; methodology: MB, VS, and SP; software: GG; investigation: MB, VS, and SP; formal analysis: MB and VS; writing—original draft: MB, VS, and SP; writing—review and editing: MB, VS, PF, CG, GG, TM, and SP; visualization: MB, VS and TM; supervision: VS, CG, and SP; funding acquisition: CG, PF, and SP.

**Funding** The work was supported by the University of Rome ‘Foro Italico’, Italy, grant to Sabrina Pitzalis (CDR2.FFABR), and by the University of Bologna (MIUR-PRIN 2017 KZNZLN).

**Availability of data and materials** Present data will be made available on request in compliance with the requirements of the funding institutes, and with the institutional ethics approval.

## Declarations

**Conflict of interest** The authors declare that they have no known competing financial interests or personal relationships that could have appeared to influence the work reported in this paper.

**Ethical approval** This study was performed in line with the principles of the Declaration of Helsinki. Approval was granted by the ethics committee at Fondazione Santa Lucia in Rome (Date: 2014; No CE/PROG:441).

**Consent to participate** Informed consent was obtained from all individual participants included in the study.

## References

- Aedo-Jury F, Cottureau BR, Celebrini S, Séverac Cauquil A (2020) Antero-Posterior vs. lateral vestibular input processing in human visual cortex. *Front Integr Neurosci* 14:43. <https://doi.org/10.3389/fnint.2020.00043>
- Andersen RA, Cui H (2009) Intention, action planning, and decision making in parietal-frontal circuits. *Neuron* 63(5):568–583. <https://doi.org/10.1016/j.neuron.2009.08.028>
- Billington J, Smith AT (2015) Neural mechanisms for discounting head-roll-induced retinal motion. *J Neurosci* 35(12):4851–4856. <https://doi.org/10.1523/JNEUROSCI.3640-14.2015>
- Buckner RL, Krienen FM, Yeo BTT (2013) Opportunities and limitations of intrinsic functional connectivity MRI. *Nat Neurosci* 16(7):832–837. <https://doi.org/10.1038/nn.3423>
- Caminiti R, Chafee MV, Battaglia-Mayer A, Averbach BB, Crowe DA, Georgopoulos AP (2010) Understanding the parietal lobe syndrome from a neurophysiological and evolutionary perspective: neurobiology and evolution of parietal cortex. *Eur J Neurosci* 31(12):2320–2340. <https://doi.org/10.1111/j.1460-9568.2010.07291.x>
- Cardin V, Smith AT (2010) Sensitivity of human visual and vestibular cortical regions to egomotion-compatible visual stimulation. *Cereb Cortex* 20(8):1964–1973. <https://doi.org/10.1093/cercor/bhp268>
- Cheng Z, Gu Y (2018) Vestibular system and self-motion. *Front Cell Neurosci* 12:456. <https://doi.org/10.3389/fncel.2018.00456>
- Cottureau BR, Smith AT, Rima S, Fize D, Héjja-Brichard Y, Renaud L, Lejards C, Vayssière N, Trotter Y, Durand J-B (2017) Processing of egomotion-consistent optic flow in the rhesus macaque cortex. *Cereb Cortex* 27:330–343. <https://doi.org/10.1093/cercor/bhw412>
- Dale AM, Fischl B, Sereno MI (1999) Cortical surface-based analysis. *Neuroimage* 9(2):179–194. <https://doi.org/10.1006/nimg.1998.0395>
- Desikan RS, Ségonne F, Fischl B, Quinn BT, Dickerson BC, Blacker D, Buckner RL, Dale AM, Maguire RP, Hyman BT, Albert MS, Killiany RJ (2006) An automated labeling system for subdividing the human cerebral cortex on MRI scans into gyral based regions of interest. *Neuroimage* 31(3):968–980. <https://doi.org/10.1016/j.neuroimage.2006.01.021>
- Di Marco S, Fattori P, Galati G, Galletti C, Lappe M, Maltempo T, Serra C, Sulpizio V, Pitzalis S (2021a) Preference for locomotion-compatible curved paths and forward direction of self-motion in

- somatomotor and visual areas. *Cortex* 137:74–92. <https://doi.org/10.1016/j.cortex.2020.12.021>
- Di Marco S, Sulpizio V, Bellagamba M, Fattori P, Galati G, Galletti C, Lappe M, Maltempo T, Pitzalis S (2021b) Multisensory integration in cortical regions responding to locomotion-related visual and somatomotor signals. *Neuroimage* 244:118581. <https://doi.org/10.1016/j.neuroimage.2021.118581>
- Field DT, Biagi N, Inman LA (2020) The role of the ventral intraparietal area (VIP/pVIP) in the perception of object-motion and self-motion. *Neuroimage* 213:116679. <https://doi.org/10.1016/j.neuroimage.2020.116679>
- Filimon F (2010) Human cortical control of hand movements: parieto-frontal networks for reaching, grasping, and pointing. *Neuroscientist* 16(4):388–407. <https://doi.org/10.1177/1073858410375468>
- Filimon F, Nelson JD, Huang R-S, Sereno MI (2009) Multiple parietal reach regions in humans: cortical representations for visual and proprioceptive feedback during on-line reaching. *J Neurosci* 29(9):2961–2971. <https://doi.org/10.1523/JNEUROSCI.3211-08.2009>
- Fischer E, Bühlhoff HH, Logothetis NK, Bartels A (2012) Human areas V3A and V6 compensate for self-induced planar visual motion. *Neuron* 73(6):1228–1240. <https://doi.org/10.1016/j.neuron.2012.01.022>
- Fischl B, Sereno MI, Dale AM (1999a) Cortical surface-based analysis. *Neuroimage* 9(2):195–207. <https://doi.org/10.1006/nimg.1998.0396>
- Fischl B, Sereno MI, Tootell RBH, Dale AM (1999b) High-resolution intersubject averaging and a coordinate system for the cortical surface. *Hum Brain Mapp* 8(4):272–284. [https://doi.org/10.1002/\(sici\)1097-0193\(1999\)8:4%3c272::aid-hbm10%3e3.0.co;2-4](https://doi.org/10.1002/(sici)1097-0193(1999)8:4%3c272::aid-hbm10%3e3.0.co;2-4)
- Frank SM, Greenlee MW (2018) The parieto-insular vestibular cortex in humans: more than a single area? *J Neurophysiol* 120(3):1438–1450. <https://doi.org/10.1152/jn.00907.2017>
- Frank SM, Sun L, Forster L, Tse PU, Greenlee MW (2016a) Cross-modal attention effects in the vestibular cortex during attentive tracking of moving objects. *J Neurosci* 36(50):12720–12728. <https://doi.org/10.1523/JNEUROSCI.2480-16.2016>
- Frank SM, Wirth AM, Greenlee MW (2016b) Visual-vestibular processing in the human Sylvian fissure. *J Neurophysiol* 116(2):263–271. <https://doi.org/10.1152/jn.00009.2016>
- Friston KJ, Buechel C, Fink GR, Morris J, Rolls E, Dolan RJ (1997) Psychophysiological and modulatory interactions in neuroimaging. *Neuroimage* 6(3):218–229. <https://doi.org/10.1006/nimg.1997.0291>
- Furlan M, Wann JP, Smith AT (2014) A representation of changing heading direction in human cortical areas pVIP and CSv. *Cereb Cortex* 24(11):2848–2858. <https://doi.org/10.1093/cercor/bht132>
- Galati G, Committeri G, Pitzalis S, Pelle G, Patria F, Fattori P, Galletti C (2011) Intentional signals during saccadic and reaching delays in the human posterior parietal cortex: Intention-related activity in the human PPC. *Eur J Neurosci* 34(11):1871–1885. <https://doi.org/10.1111/j.1460-9568.2011.07885.x>
- Galati G, Committeri G, Spitoni G, Aprile T, Di Russo F, Pitzalis S, Pizzamiglio L (2008) A selective representation of the meaning of actions in the auditory mirror system. *Neuroimage* 40(3):1274–1286. <https://doi.org/10.1016/j.neuroimage.2007.12.044>
- Galletti C, Battaglini PP, Fattori P (1990) ‘Real-motion’ cells in area V3A of macaque visual cortex. *Exp Brain Res* 82(1):67–76. <https://doi.org/10.1007/BF00230838>
- Galletti C, Fattori P (2003) Neuronal mechanisms for detection of motion in the field of view. *Neuropsychologia* 41(13):1717–1727. [https://doi.org/10.1016/S0028-3932\(03\)00174-X](https://doi.org/10.1016/S0028-3932(03)00174-X)
- Galletti C, Fattori P (2018) The dorsal visual stream revisited: Stable circuits or dynamic pathways? *Cortex* 98:203–217. <https://doi.org/10.1016/j.cortex.2017.01.009>
- Galletti C, Gamberini M, Kutz DF, Fattori P, Luppino G, Matelli M (2001) The cortical connections of area V6: An occipito-parietal network processing visual information: cortical connections of area V6. *Eur J Neurosci* 13(8):1572–1588. <https://doi.org/10.1046/j.0953-816x.2001.01538.x>
- Gibson JJ (1950) *The perception of the visual world*. Houghton Mifflin, Boston
- Glasser MF, Sotiropoulos SN, Wilson JA, Coalson TS, Fischl B, Andersson JL, Xu J, Jbabdi S, Webster M, Polimeni JR, Van Essen DC, Jenkinson M (2013) The minimal preprocessing pipelines for the human connectome project. *Neuroimage* 80:105–124. <https://doi.org/10.1016/j.neuroimage.2013.04.127>
- Graziano MS, Gross CG (1998) Spatial maps for the control of movement. *Curr Opin Neurobiol* 8(2):195–201. [https://doi.org/10.1016/S0959-4388\(98\)80140-2](https://doi.org/10.1016/S0959-4388(98)80140-2)
- Greenlee MW, Frank SM, Kaliuzhna M, Blanke O, Bremmer F, Churan J, Cuturi LF, MacNeilage PR, Smith AT (2016) Multisensory integration in self motion perception. *Multisens Res* 29(6–7):525–556. <https://doi.org/10.1163/22134808-00002527>
- Hagler DJ, Riecke L, Sereno MI (2007) Parietal and superior frontal visuospatial maps activated by pointing and saccades. *Neuroimage* 35(4):1562–1577. <https://doi.org/10.1016/j.neuroimage.2007.01.033>
- Heed T, Beurze SM, Toni I, Roder B, Medendorp WP (2011) Functional rather than effector-specific organization of human posterior parietal cortex. *J Neurosci* 31(8):3066–3076. <https://doi.org/10.1523/JNEUROSCI.4370-10.2011>
- Heed T, Leone FTM, Toni I, Medendorp WP (2016) Functional versus effector-specific organization of the human posterior parietal cortex: revisited. *J Neurophysiol* 116(4):1885–1899. <https://doi.org/10.1152/jn.00312.2014>
- Huang R-S, Chen C, Sereno MI (2015) Neural substrates underlying the passive observation and active control of translational egomotion. *J Neurosci* 35(10):4258–4267. <https://doi.org/10.1523/JNEUROSCI.2647-14.2015>
- Huang R-S, Chen C, Tran AT, Holstein KL, Sereno MI (2012) Mapping multisensory parietal face and body areas in humans. *Proc Natl Acad Sci* 109(44):18114–18119. <https://doi.org/10.1073/pnas.1207946109>
- Huang R-S, Sereno MI (2007) Dodecapus: An MR-compatible system for somatosensory stimulation. *Neuroimage* 34(3):1060–1073. <https://doi.org/10.1016/j.neuroimage.2006.10.024>
- Huang R-S, Sereno MI (2018) Multisensory and sensorimotor maps. *Handb Clin Neurol* 151:141–161. <https://doi.org/10.1016/B978-0-444-63622-5.00007-3>
- Kwong KK, Belliveau JW, Chesler DA, Goldberg IE, Weisskoff RM, Poncelet BP, Kennedy DN, Hoppel BE, Cohen MS, Turner R (1992) Dynamic magnetic resonance imaging of human brain activity during primary sensory stimulation. *Proc Natl Acad Sci* 89(12):5675–5679. <https://doi.org/10.1073/pnas.89.12.5675>
- Leone FTM, Heed T, Toni I, Medendorp WP (2014) Understanding effector selectivity in human posterior parietal cortex by combining information patterns and activation measures. *J Neurosci* 34(21):7102–7112. <https://doi.org/10.1523/JNEUROSCI.5242-13.2014>
- Limanowski J, Lopes P, Keck J, Baudisch P, Friston K, Blankenburg F (2019) Action-dependent processing of touch in the human parietal operculum and posterior insula. *Cereb Cortex* 30:607–617. <https://doi.org/10.1093/cercor/bhz111>
- Maltempo T, Pitzalis S, Bellagamba M, Di Marco S, Fattori P, Galati G, Galletti C, Sulpizio V (2021) Lower visual field preference for the visuomotor control of limb movements in the human dorsomedial parietal cortex. *Brain Struct Funct* 226(9):2989–3005. <https://doi.org/10.1007/s00429-021-02254-3>

- McLaren DG, Ries ML, Xu G, Johnson SC (2012) A generalized form of context-dependent psychophysiological interactions (gPPI): a comparison to standard approaches. *Neuroimage* 61(4):1277–1286. <https://doi.org/10.1016/j.neuroimage.2012.03.068>
- Medendorp WP, Heed T (2019) State estimation in posterior parietal cortex: distinct poles of environmental and bodily states. *Prog Neurobiol* 183:101691. <https://doi.org/10.1016/j.pneurobio.2019.101691>
- Nau M, Schindler A, Bartels A (2018) Real-motion signals in human early visual cortex. *Neuroimage* 175:379–387. <https://doi.org/10.1016/j.neuroimage.2018.04.012>
- Oldfield RC (1971) The assessment and analysis of handedness: The Edinburgh inventory. *Neuropsychologia* 9(1):97–113. [https://doi.org/10.1016/0028-3932\(71\)90067-4](https://doi.org/10.1016/0028-3932(71)90067-4)
- Orban GA (2008) Higher order visual processing in macaque extrastriate cortex. *Physiol Rev*. <https://doi.org/10.1152/physrev.00008.2007>
- Pitzalis S, Fattori P, Galletti C (2015) The human cortical areas V6 and V6A. *Vis Neurosci* 32:E007. <https://doi.org/10.1017/S0952523815000048>
- Pitzalis S, Galletti C, Huang R-S, Patria F, Committeri G, Galati G, Fattori P, Sereno MI (2006) Wide-field retinotopy defines human cortical visual area V6. *J Neurosci* 26(30):7962–7973. <https://doi.org/10.1523/JNEUROSCI.0178-06.2006>
- Pitzalis S, Hadj-Bouziane F, Dal Bò G, Guedj C, Strappini F, Meunier M, Farnè A, Fattori P, Galletti C (2021) Optic flow selectivity in the macaque parieto-occipital sulcus. *Brain Struct Funct* 6:91. <https://doi.org/10.1007/s00429-021-02293-w>
- Pitzalis S, Sdoia S, Bultrini A, Committeri G, Di Russo F, Fattori P, Galletti C, Galati G (2013a) Selectivity to translational egomotion in human brain motion areas. *PLoS ONE* 8(4):e60241. <https://doi.org/10.1371/journal.pone.0060241>
- Pitzalis S, Sereno MI, Committeri G, Fattori P, Galati G, Patria F, Galletti C (2010) Human V6: the medial motion area. *Cereb Cortex* 20(2):411–424. <https://doi.org/10.1093/cercor/bhp112>
- Pitzalis S, Sereno MI, Committeri G, Fattori P, Galati G, Tosoni A, Galletti C (2013b) The human homologue of macaque area V6A. *Neuroimage* 82:517–530. <https://doi.org/10.1016/j.neuroimage.2013.06.026>
- Pitzalis S, Serra C, Sulpizio V, Committeri G, Pasquale F, Fattori P, Galletti C, Sepe R, Galati G (2020) Neural bases of self- and object-motion in a naturalistic vision. *Hum Brain Mapp* 41(4):1084–1111. <https://doi.org/10.1002/hbm.24862>
- Pitzalis S, Serra C, Sulpizio V, Di Marco S, Fattori P, Galati G, Galletti C (2019) A putative human homologue of the macaque area PEc. *Neuroimage* 202:116092. <https://doi.org/10.1016/j.neuroimage.2019.116092>
- Power JD, Barnes KA, Snyder AZ, Schlaggar BL, Petersen SE (2012) Spurious but systematic correlations in functional connectivity MRI networks arise from subject motion. *Neuroimage* 59(3):2142–2154. <https://doi.org/10.1016/j.neuroimage.2011.10.018>
- Schindler A, Bartels A (2018) Integration of visual and non-visual self-motion cues during voluntary head movements in the human brain. *Neuroimage* 172:597–607. <https://doi.org/10.1016/j.neuroimage.2018.02.006>
- Sereno MI, Huang R-S (2006) A human parietal face area contains aligned head-centered visual and tactile maps. *Nat Neurosci* 9(10):1337–1343. <https://doi.org/10.1038/nn1777>
- Sereno MI, Pitzalis S, Martínez A (2001) Mapping of contralateral space in retinotopic coordinates by a parietal cortical area in humans. *Science* 294(5545):1350–1354. <https://doi.org/10.1126/science.1063695>
- Serra C, Galletti C, Di Marco S, Fattori P, Galati G, Sulpizio V, Pitzalis S (2019) Egomotion-related visual areas respond to activeleg movements. *Hum Brain Mapp* 40(11):3174–3191. <https://doi.org/10.1002/hbm.24589>
- Smith AT (2021) Cortical visual area CSv as a cingulate motor area: a sensorimotor interface for the control of locomotion. *Brain Struct Funct* 226(9):2931–2950. <https://doi.org/10.1007/s00429-021-02325-5>
- Smith AT, Beer AL, Furlan M, Mars RB (2018) Connectivity of the cingulate sulcus visual area (CSv) in the human cerebral cortex. *Cereb Cortex* 28(2):713–725. <https://doi.org/10.1093/cercor/bhx002>
- Smith AT, Greenlee MW, DeAngelis GC, Angelaki DE (2017) Distributed visual-vestibular processing in the cerebral cortex of man and macaque. *Multisens Res* 30(2):91–120. <https://doi.org/10.1163/22134808-00002568>
- Smith AT, Wall MB, Thilo KV (2012) Vestibular inputs to human motion-sensitive visual cortex. *Cereb Cortex* 22(5):1068–1077. <https://doi.org/10.1093/cercor/bhr179>
- Sulpizio V, Galati G, Fattori P, Galletti C, Pitzalis S (2020) A common neural substrate for processing scenes and egomotion-compatible visual motion. *Brain Struct Funct* 225(7):2091–2110. <https://doi.org/10.1007/s00429-020-02112-8>
- Tootell RBH, Mendola JD, Hadjikhani NK, Ledden PJ, Liu A, K., Reppas, J. B., Sereno, M. I., & Dale, A. M. (1997) Functional analysis of V3A and related areas in human visual cortex. *J Neurosci* 17(18):7060–7078. <https://doi.org/10.1523/JNEUROSCI.17-18-07060.1997>
- Tosoni A, Pitzalis S, Committeri G, Fattori P, Galletti C, Galati G (2015) Resting-state connectivity and functional specialization in human medial parieto-occipital cortex. *Brain Struct Funct* 220(6):3307–3321. <https://doi.org/10.1007/s00429-014-0858-x>
- Van Essen DC, Ugurbil K, Auerbach E, Barch D, Behrens TEJ, Bucholz R, Chang A, Chen L, Corbetta M, Curtiss SW, Della Penna S, Feinberg D, Glasser MF, Harel N, Heath AC, Larson-Prior L, Marcus D, Michalareas G, Moeller S, Yacoub E (2012) The Human connectome project: a data acquisition perspective. *Neuroimage* 62(4):2222–2231. <https://doi.org/10.1016/j.neuroimage.2012.02.018>
- Wall MB, Smith AT (2008) The Representation of egomotion in the human brain. *Curr Biol* 18(3):191–194. <https://doi.org/10.1016/j.cub.2007.12.053>
- Warren PA, Rushton SK (2009) Optic flow processing for the assessment of object movement during ego movement. *Curr Biol* 19(18):1555–1560. <https://doi.org/10.1016/j.cub.2009.07.057>

**Publisher's Note** Springer Nature remains neutral with regard to jurisdictional claims in published maps and institutional affiliations.